

EXPERIMENTAL INVESTIGATION ON PUNCHING BEHAVIOR
OF THICK REINFORCED CONCRETE SLABST. URBAN¹, M. GOŁDYN², J. KRAKOWSKI³, Ł. KRAWCZYK⁴

The results of experimental test of nine thickset reinforced concrete slabs in punching are presented in the this paper. The aim of the-tests was verification of the Eurocode EC 2 procedure, by which the ultimate shear stresses $v_{Rd,c}$ depend on the slenderness of the slab. Besides of the performed tests results, the analysis of the foreign investigation of the fundamentals is also included. The test results, as well as other tests, show the correctness of the function assumed in Eurocode 2, which gives correlation between ultimate stresses $v_{Rd,c}$ and shear slenderness.

Key words: concrete, punching shear, shear slenderness, slab, ultimate shear stress

1. INTRODUCTION

Slenderness of a floor slab in standard frame constructions of a slab column type, defined as the span to the thickness of the floor ratio (l/h), usually ranges from 20 to 30. Apart from the slenderness of a floor understood in such a way, the shear slenderness of a slab is also presented in the literature by the formula:

$$(1.1) \quad \lambda = \frac{L - c}{2d},$$

where: L – is a diameter of the field of negative radial moments in the support zone (with a distance between the central line of supports taken from the relevant model from experimental investigations), c – is the column cross sectional dimension, d – is the effective depth of the slab. Details of symbols are clarified in Fig. 1. The shear slenderness ratio λ ranges from 5 to 7.5 for standard floor slabs, assuming that L is diameter of a circle where radial moments equal zero.

¹ Prof. PhD Eng., Department of Concrete Structures, Lodz University of Technology, Poland. e-mail: tadasz.urban@p.lodz.pl

² M.Sc Eng., Department of Concrete Structures, Lodz University of Technology, Poland. e-mail: michal.goldyn@p.lodz.pl

³ M.Sc Eng., Department of Concrete Structures, Lodz University of Technology, Poland. e-mail: jakub.krakowski@p.lodz.pl

⁴ M.Sc Eng., Department of Concrete Structures, Lodz University of Technology, Poland. e-mail: lukasz.krawczyk@p.lodz.pl

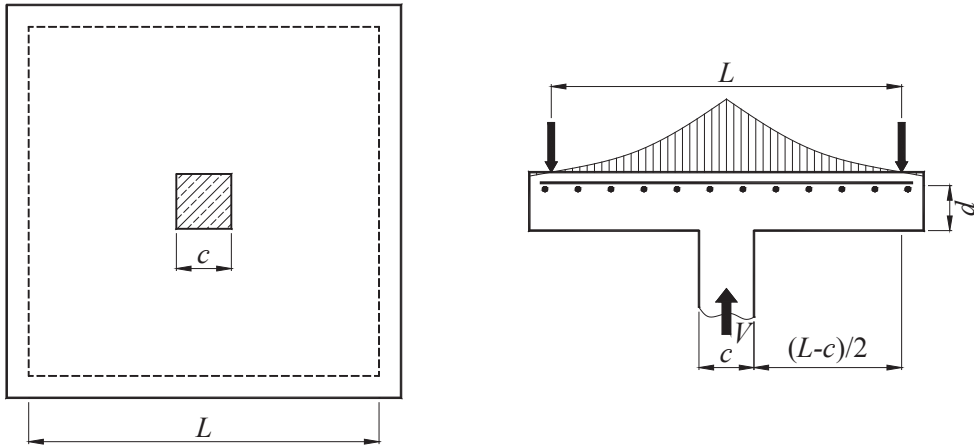


Fig. 1. Definition of the shear slenderness

The experimental verification of this problem is presented by Lovrovich and McLean [1]. They made two series of five models of circular slabs, in which a span to the thickness of the slab ratio was a variable parameter. In one of the series, the slabs were reinforced for shear. The thickness of slab was $h \approx 102$ mm ($d \approx 83$ mm), the ratio of main reinforcement was $\rho_l = 1.75\%$ ($\varnothing \approx 9.5$ mm, $f_y = 531$ MPa). The shear reinforcement was made of 3.73 mm diameter ribbed bars in the form of single-arm stirrups, and the yield strength was approximately about $f_{yw} = 280$ MPa. The ends of the stirrups were bent on the outside layer of bars of the bottom and upper mesh of main reinforcement. The load was applied by means of a cylinder of 101.6 mm diameter. The graphs in Fig. 2 show shear stress in the control section located at a distance of $d/2$ from the face of the column in the function of the shear slenderness λ . In spite of small scale of the models, the results of this experiment confirm that the influence of the shear slenderness on the punching capacity is analogous to such an influence which occurs in concrete beams.

As in standard inter-story floors, the shear slenderness is too high ($\lambda > 3$), therefore it cannot have any significant effect on punching capacity. In case of thick slabs (e.g. footing slabs) and pad foundation, the situation is different. Eurocode 2 [2] takes into account the problem of shear slenderness for such cases by introducing modification to the basic calculation procedure. Eurocode 2 requires checking the shear resistance at perimeters situated between perimeter u_1 at a distance $2,0d$ from the column face, and perimeter u_0 which is at the joint with the column. Moreover, the punching force can be reduced by the value of soil resistance under the section of foundation effecting within the analysed control perimeter.

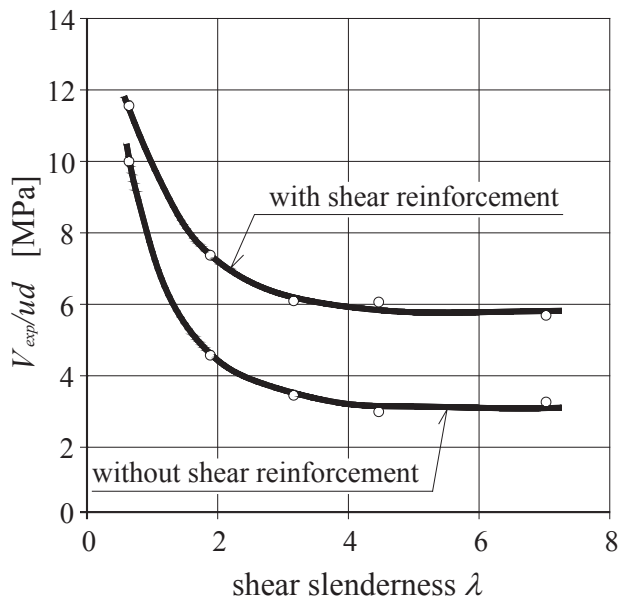


Fig. 2. Influence of the shear slenderness on the punching capacity by Lovrovich's and Mc Lean's [1] investigations

The aim of this investigation is to verify the normalization dependence (2), which is used to determine the limit of shear stress on the length of the analysed control circuit:

$$(1.2) \quad v_{Rc} = 0,18 \cdot k \cdot \sqrt[3]{100 \rho_l f_{ck}} \cdot \frac{2d}{a},$$

$$(1.3) \quad v_{Rc} \geq v_{\min} \frac{2d}{a} = 0,035 \sqrt{k^3 f_{ck}} \cdot \frac{2d}{a},$$

in which: k – is the scale factor ($k = 1 + \sqrt{200/d} \leq 2,0$, d in [mm]), ρ_l – average reinforcement ratio for main longitudinal reinforcement, f_{ck} – characteristic compressive strength of concrete [MPa], d – effective depth of slab, a – distance between the column face to the control perimeter u . By comparing this equation with formula used to determine the shear stresses in the floor slab (of slender slab) it is possible to notice in (2) an additional function $f(a) = 2d/a$ which takes into account the effect of shear slenderness. This additional component is causing a very significant increase in the maximum stress, when the control perimeter u is closer to the column. Ultimate stress at the perimeter located at a distance $a = d$ is twice as big as at the basic perimeter u_1 .

2. PREVIOUS RESEARCH

The first experimental investigation on pad footings was undertaken by Talbot [3] in 1909-1912 at the Illinois University. These examinations were carried on models made of contemporary materials – concrete of relatively low compressive strength and smooth rebars. Some elements were destroyed as a result of loss of main reinforcement adhesion – “diagonal tension failure”.

Investigations [3] in Illinois were continued in 1944÷1948 by Richart [4]. One of the conclusions of that research was that the increase in the effective depth of foundation resulted in reduction of shear stresses.

In the years 1967÷1980 in Otto Graf Institute in Stuttgart, Dieterle [5] studied pad footings, with the aim to determine the influence on the capacity of such factors as: reinforcement ratio for the main reinforcement, geometry and shear slenderness. It was found that the introduction of large amounts of main reinforcement was is pointless, because it was not fully utilized. It was noticed that at the state of destruction, the shear stress in thick slabs was significantly lower than that in the thin and slender ones.

In 1998 Hallgren, Kinnunen and Nylander [6] presented the results of their experimental investigations on thickset slabs. The research was to test the effect of factors such as: strength of the concrete, ratio of flexural reinforcement, way of the anchorage of flexural reinforcement, usage and type of shear reinforcement, method of applying loading and shapes of the slabs. The conclusions of these studies can be summarized in the following statements: the angle of diagonal cracks ranges between 50° to 60° ; the strength of concrete has a significant impact on the punching capacity; the ultimate shear stress increases with the strength of concrete to a greater extent than it is in the case of slender slabs, the punching capacity increases slightly with an increase of flexural reinforcement, the type of a load applied, e.g. the concentrated load or uniform load, does not affect the strength of punching, the slab shape (square, round) does not affect the strength of the destructive load.

Timm’s studies [7] included numerical analysis and some experimental investigations on punching capacity of pad footing. The conclusions of the study can be summarized as follows: stocky slabs are damaged as a result of diagonal cracks which cross the compression zone, the column cross sectional dimension has a significant impact on the capacity, the ratio of flexural reinforcement has little effect on capacity. Shear reinforcement delays the process of the inclined cracks becoming destructive ones.

Hegger, Sherif and Ricker’s research [8], [9] is very important for the considered problem. This research was performed in conditions similar to the real life models, and was carried out on pad footing supported on sand, or pressure was exerted on footing with many points using hydraulic press. The results of these studies led to the following conclusions:

- The inclination of the failure shear crack seems to be mainly influenced by a/d , where a is the reach of the foot cantilever (the observed inclinations of the failure

crack were approximately 45° for compact footings with $a/d = 1,25$ and less than 35° for more slender footings with $a/d = 2,0$;

- The punching shear resistance is strongly influenced by a/d (the shear strength decreases with increase of a/d);
- Shear reinforcement can substantially increase the punching capacity of footings but is less effective with decreasing of a/d ;
- The footing supported off sand showed higher punching shear resistance than those uniformly loaded by means of hydraulic cylinders. This may be attributed to the soil pressure concentration underneath the footing.

3. OWN RESEARCH

3.1. EXPERIMENTAL PROGRAM

The main aim of the research was to verify the equation (2), and in principle adopted in the formula method of including the shear slenderness of slab as a function $f(a) = 2d/a$. The quotient expresses an angle of diagonal cracks θ in the ultimate limit state. In order to achieve variation of the angle θ in the tested models, the effective depth of slab d was taken as the primary variable parameter. The research was carried out on a special test bed, which is shown in Fig. 3.

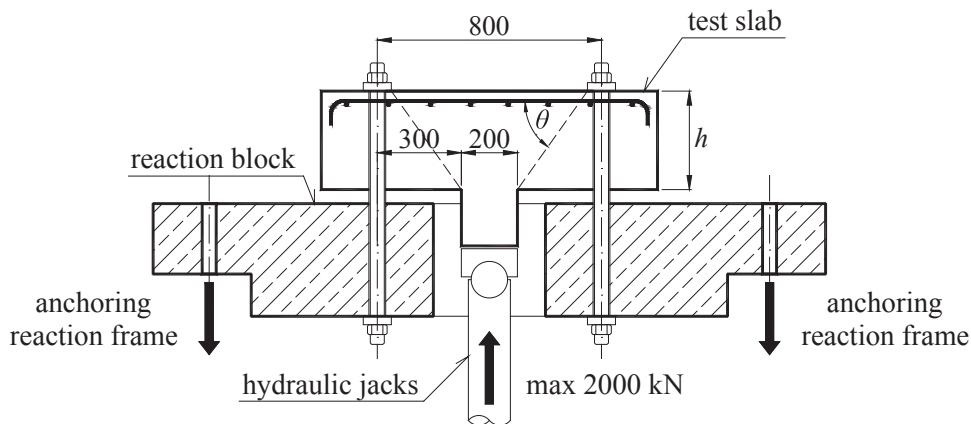


Fig. 3. Test set-up

The paper presents the results of 9 models, performed in two series of research. The models of the series were made of the same concrete mix. Concrete compressive strength was monitored by testing cylinder samples (diameter of 150 mm and a height of 300 mm). The models were in the shape of octagonal slab with a centrally located

column of 200 mm diameter. The columns were made of high-strength concrete of approximately 90 MPa. Other parameters of tested models are presented in Table 1.

Fig. 4 and 5 show examples of models reinforcement. In the first series the same reinforcement bars 8 mm diameter were used in all models what resulted in diversity in flexural reinforcement ratio. In the second series flexural reinforcement ratio was constant (around 0.4%). This necessitated use of various diameters bars.

Table 1

Parameters of the investigated specimens

Research series	Model	h	d	ρ_l	f_{ym}	f_{cm}	V_{exp}
		[mm]		[%]	[MPa]	[MPa]	[kN]
1	P-15-0.32	150	118	0.32	565	27.0	270
	P-20-0.21	200	168	0.21	565	26.2	390
	P-25-0.17	250	218	0.17	565	29.0	480
	P-30-0.14	300	268	0.14	565	29.0	620
	P-35-0.12	350	318	0.12	565	31.0	740
2	P-20-0.40	200	168	0.40	565	32.5	660
	P-25-0.40	250	218	0.40	544	32.5	920
	P-30-0.40	300	268	0.40	544	32.5	1280
	P-35-0.40	350	318	0.40	580	32.5	2000

h – thickness of the slab, d – average effective depth of slab, ρ_l – the average ratio of flexural reinforcement, f_{ym} yield point of the reinforcement, f_{cm} – compressive strength of concrete, V_{exp} – experimental capacity.

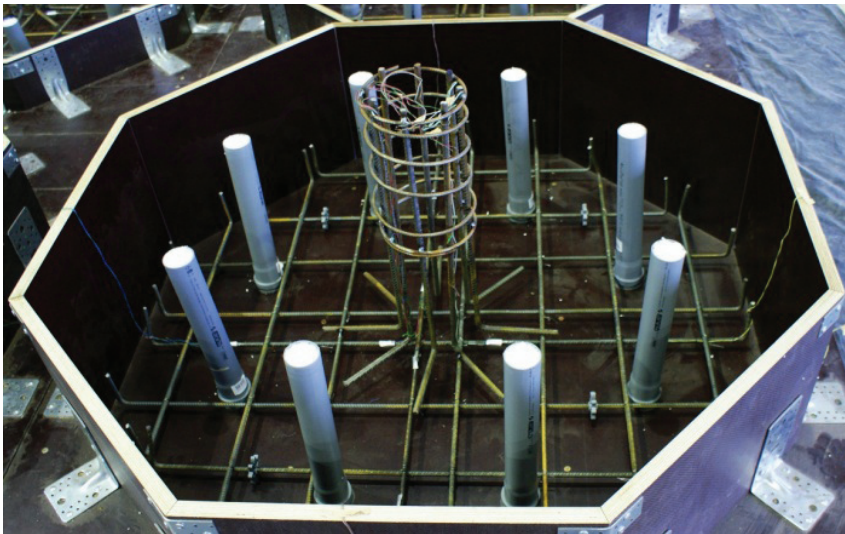


Fig. 4. Reinforcement of model P-35-0.12 (first series)

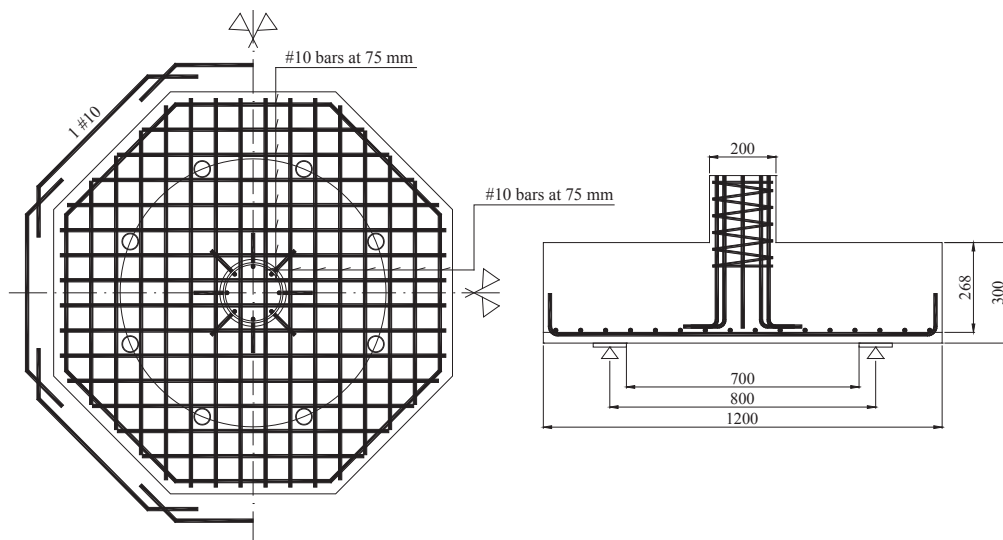


Fig. 5. Reinforcement of model P-30-0.40 (second series)

The test models were connected to the test bed by eight screws. In the first series the screws were tightened on the tension surface of the model, and at each nut a metal washers 100 x 150 mm were provided (Fig. 6a). In the second series the locking screws were modified, as shown in Fig. 6b. This steel flange consisted of 8 independent segments and was aimed at forcing the precise location of the outlet diagonal cracks. The loading on the models was applied by means of the series of four hydraulic cylinders to give maximum pressure of 2000 kN. The loading was applied at the bottom of the column (Fig. 3).



Fig. 6. Types of locking slabs: a) the first series, b) the second series

During the study the following measurements were taken:

- the radial compression strains of the concrete surface in the vicinity of the column, measured by gauges of the basis of 50 mm,
- strains of the main reinforcement of slab (gauges on the basis of 10 mm),
- the propagation of cracks and their width were measured at selected locations.

Figure 7 shows the location of strain gauges.

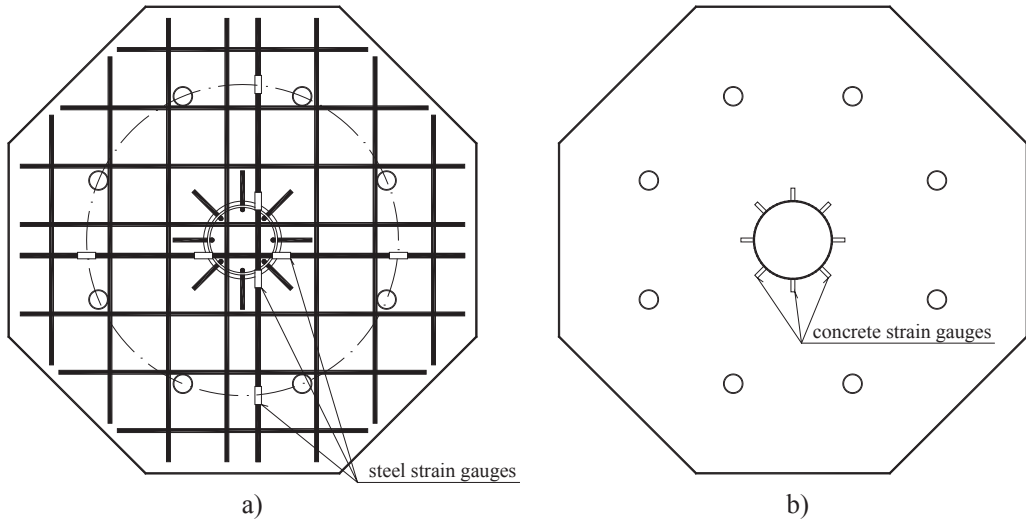


Fig. 7. Location of the electric resistance wire strain gauges:
a) on concrete, b) on reinforcement

3.2. EXPERIMENTAL RESULTS

3.2.1. Deformation of the reinforcement

Figure 8 summarizes the mean deformation of the main reinforcement of the edge of the column of the second series as a function of loading. The model P-35-0.40 after reaching the force of 1600 kN was unloaded, and the next day the test was resumed until the destruction at the loading of 2000 kN. Therefore, in fig. 8 the model P-35-0.40 is represented by two diagrams. With the exception of the P-25-.40 all models exceeded the yield point.

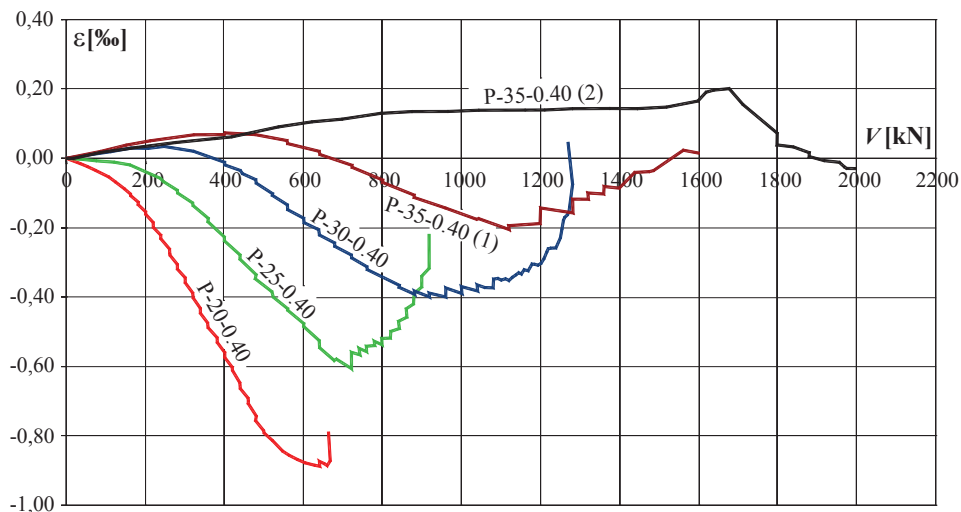


Fig. 8. The mean deformation of the main reinforcement of the edge of the column of the second series

3.2.2. Deformation of the reinforcement

Fig. 9 shows the plots of the radial compression deformation of the concrete surface in vicinity of the column. It can be seen that the thicker the slab is (reducing the slenderness), the smaller the absolute values of concrete deformation. In the case of thick slabs, even the sign of strain changes.

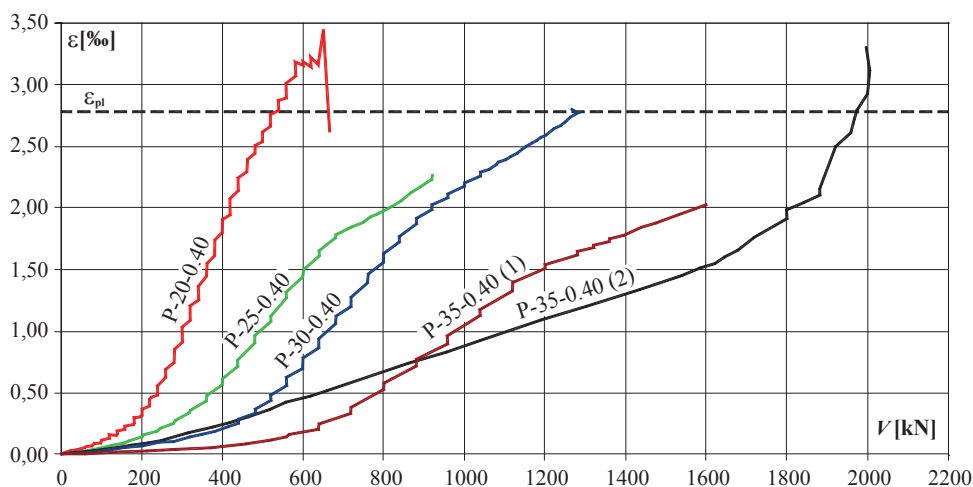


Fig. 9. The mean radial compression deformation of the concrete surface in vicinity of the column of the second series

3.2.3. Ultimate limit state

Destructive forces (V_{exp}) achieved in the study are summarized in Table 1, along with the basic geometric parameters and strength of models. The effective depth of slab was measured after the destruction of models by measuring actual concrete cover. In this way the average ratio of the main reinforcement was established.

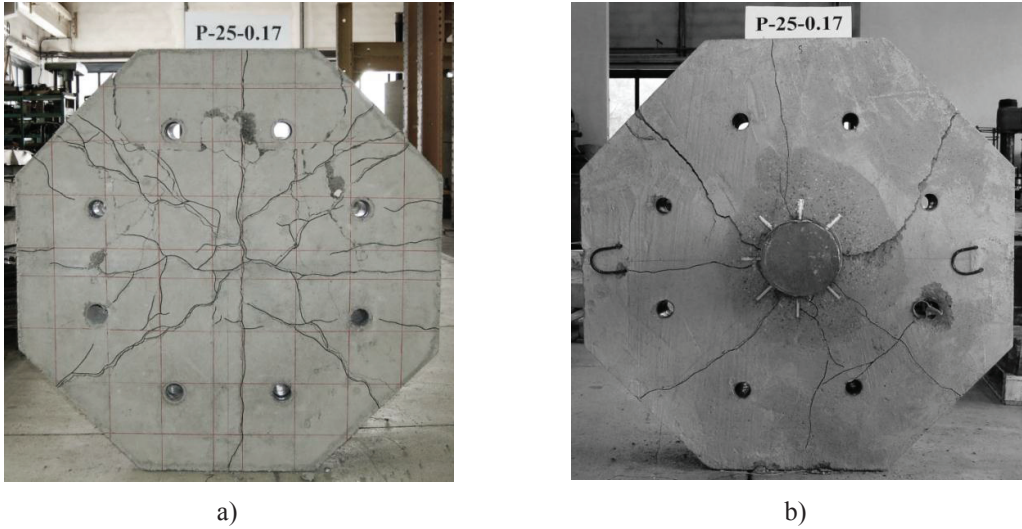


Fig. 10. View of P-25-0.17 after the test:
a) on the reinforcement side, b) on the side where load was applied



Fig. 11. Punching cone semi-exposed in P-25-0.17

The models of the first series, P-15-0.32, and P-20-0.21, were destroyed in a rapid way which is typical for punching. The diagonal cracks formed within the area defined by anchor bolts. Other models of the first series were destroyed in a different way. Creation of the punching cone was preceded by a rapid development of radial cracks, developed also on the side where the load was applied (Fig. 10). In Fig. 10a it can also be noted that the outlet of diagonal crack was irregular, and between the anchor bolts it ran out of their circle. Fig 11 shows the punching cone semi-exposed in the P-25-0.17.

The use of “rigid steel flange” in the second series forced the formation of onset of diagonal cracks on the inside edge of the flange (Fig. 12 and 13).

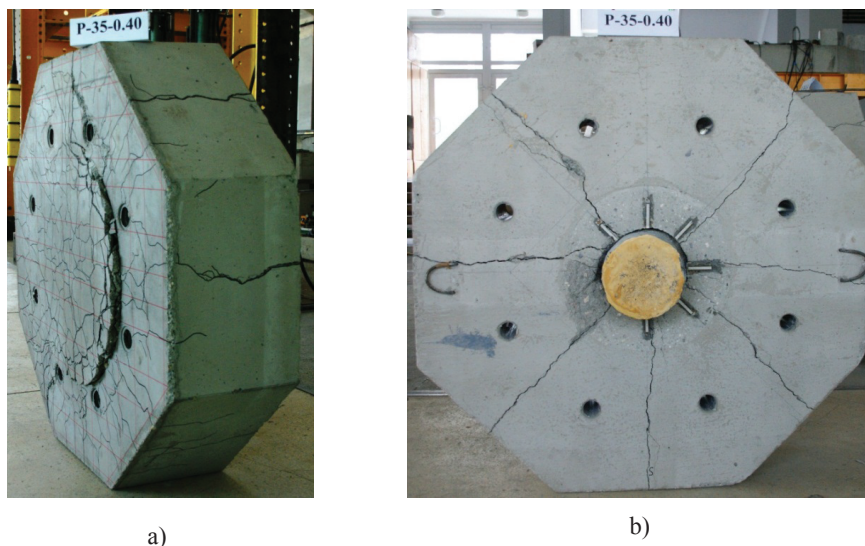


Fig. 12. Photo of P-35-0.40 after the test: a) on the reinforcement side, b) on the side where load was applied



Fig. 13. Photo of cross-section P-35-0.40 after the test

4. DISCUSSION OF EXPERIMENTAL INVESTIGATION RESULTS

The obtained experimental capacities (V_{exp}) were compared with the equation recommended by Eurocode 2 [2]. For the first series, the distance between the column face and the axis of the screw was assumed as $a_L = 300$ mm. However, in the second series, the onset of diagonal crack was determined by the inner edge of the steel flange, and it caused the intersection of the theoretical diagonal crack with the surface of the center of gravity of the main reinforcement for different values of a . Fig. 14 shows the method adopted to define distance a for the models in the second series.

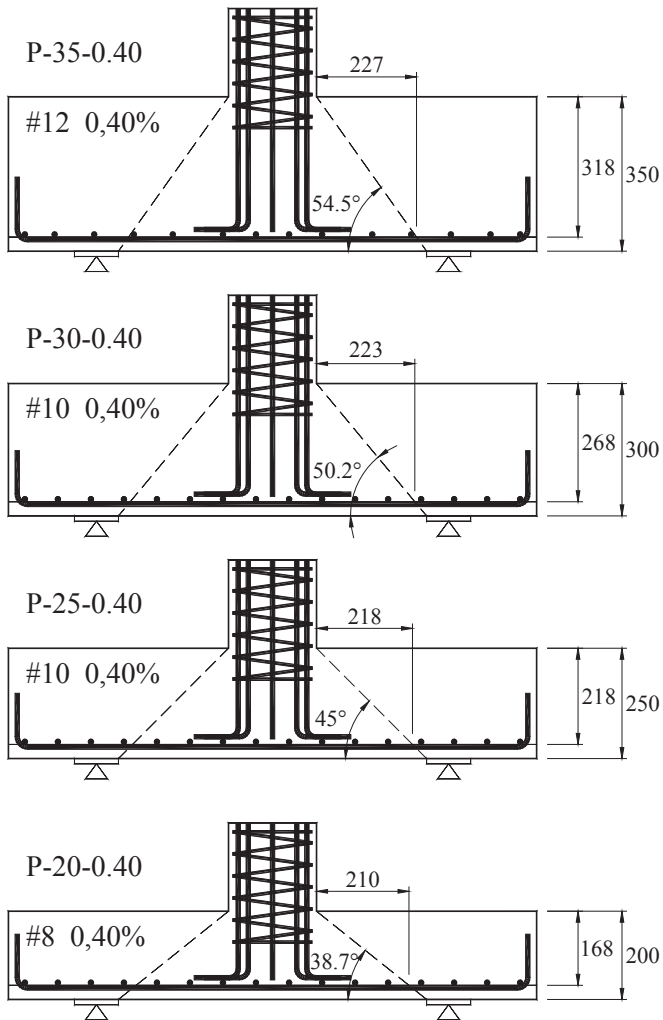


Fig. 14. The theoretical line of diagonal cracks in the second series

This analysis also included the results of studies of foundation slabs by others [6], [7]. Tables 2 and 3 show the results of the shear stresses at the control perimeter u . The tables also include a comparison of experimental shear stresses with stresses calculated in accordance with the formula (2) in which the compressive strength of concrete, was taken as an average $f_{ck} = f_{cm}$.

Table 2

Comparison of own results with Eurocode 2

Model		a	d	a/d	u	k	v_{exp}	v_{Rc}	$\frac{v_{exp}}{v_{Rc}}$
		[mm]		[-]	[mm]	[-]	[MPa]		[-]
The 1 st series	P-15-0.32	236	118	2.000	2111	2.000	1.084	0.739	1.467
	P-20-0.21	252	168	1.500	2212	2.000	1.050	0.847	1.239
	P-25-0.17	262	218	1.202	2275	1.958	0.968	0.998	0.970
	P-30-0.14	268	268	1.000	2312	1.864	1.001	1.070	0.935
	P-35-0.12	273	318	0.858	2344	1.793	0.993	1.165	0.852
The 2 nd series	P-20-0.40	210	168	1.250	1948	2.000	2.017	1.354	1.489
	P-25-0.40	218	218	1.000	1998	1.958	2.112	1.657	1.275
	P-30-0.40	223	268	0.833	2029	1.864	2.353	1.896	1.254
	P-35-0.40	227	318	0.714	2055	1.793	3.061	2.126	1.440
a – distance between the column face to the control perimeter considered, k – the size factor of the effective depth, v_{exp} – the shear stress at the periphery of the control u , v_{Rc} – stress calculated according to the formula (2)	mean						1 st series	1.093	
							2 nd series	1.361	
	standard deviation						1 st series	0.255	
							2 nd series	0.122	
	coefficient of variation						1 st series	0.233	
							2 nd series	0.089	

Table 3

Comparison of the results of foreign studies [6] and [7] with Eurocode 2

Model		a	d	a/d	u	k	v_{exp}	v_{Rc}	$\frac{v_{exp}}{v_{Rc}}$
		[mm]		[-]	[mm]	[-]	[MPa]		[-]
S1		175	242	0.723	1885	1.909	2.988	2.440	1.224
S2		175	243	0.720	1885	1.907	2.216	2.187	1.013
S3		175	250	0.700	1885	1.894	2.139	2.251	0.950
S4		175	232	0.754	1885	1.928	2.268	2.412	0.940

Table 3

Model	a	d	a/d	u	k	v_{exp}	v_{Rc}	$\frac{v_{exp}}{v_{Rc}}$	
	[mm]		[-]	[mm]	[-]	[MPa]		[-]	
S7	175	246	0.711	1885	1.902	1.341	1.760	0.762	
S8	175	245	0.714	1885	1.904	1.981	1.946	1.018	
S9	175	244	0.717	1885	1.905	1.966	2.117	0.928	
S11	175	235	0.745	1885	1.923	2.686	2.146	1.252	
S12	212	242	0.876	2117	1.909	2.047	1.805	1.134	
S13	212	244	0.869	2117	1.905	1.554	1.631	0.953	
S14	175	240	0.729	1885	1.913	2.432	1.989	1.223	
Ti-1A	192,5	172	1.119	1759	2.000	2.224	2.384	0.933	
Ti-2A	312,5	172	1.817	2513	2.000	1.545	1.410	1.096	
Ti-3A	275	242	1.136	2513	1.909	1.743	2.046	0.852	
a – distance between the column face to the control perimeter considered k – the size factor of the effective depth v_{exp} – the shear stress at the periphery of the control u , v_{Rc} – stress calculated according to the formula (2)						mean		Hallgren	1.036
								standard deviation	
						coefficient of variation			

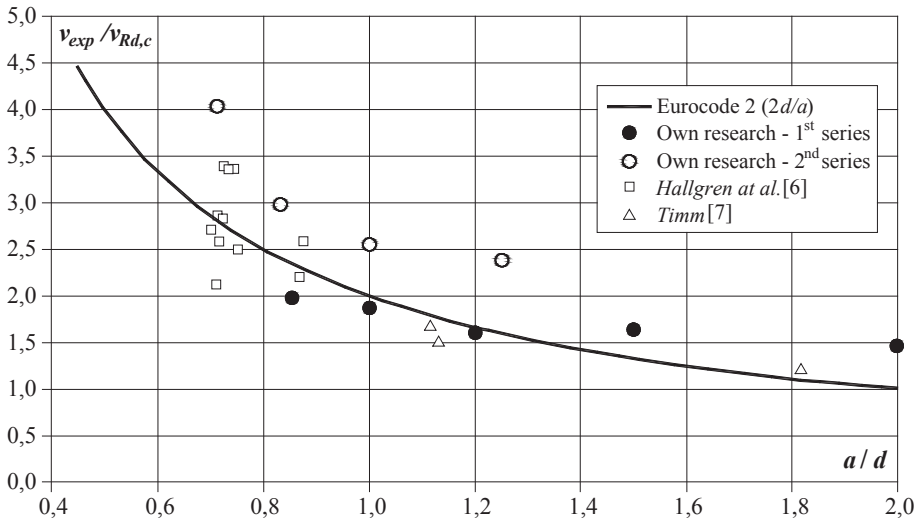


Fig. 15. The theoretical curve of the ratio $v_{R,c}/v_{exp}$ as a function of a/d

Considering the differences between the first and the second series of results, the different concept of reinforcement in each series should be also taken into consideration. That is shown in different ratio of flexural reinforcement. In the slabs of the second series, in addition to the increased ratio of flexural reinforcement, peripheral reinforcement bars were also used which hindered the deformation in the circumferential direction. Such deformations are present in real construction and they manifest by increasing capacity of the slab-column connection. This problem was studied by Rankin and Long [11], who concluded that, depending on the ratio of flexural reinforcement of the slab, the effect which is called membrane action, may increase the capacity by about 30 ÷ 50%. This effect is illustrated by Fig. 16.

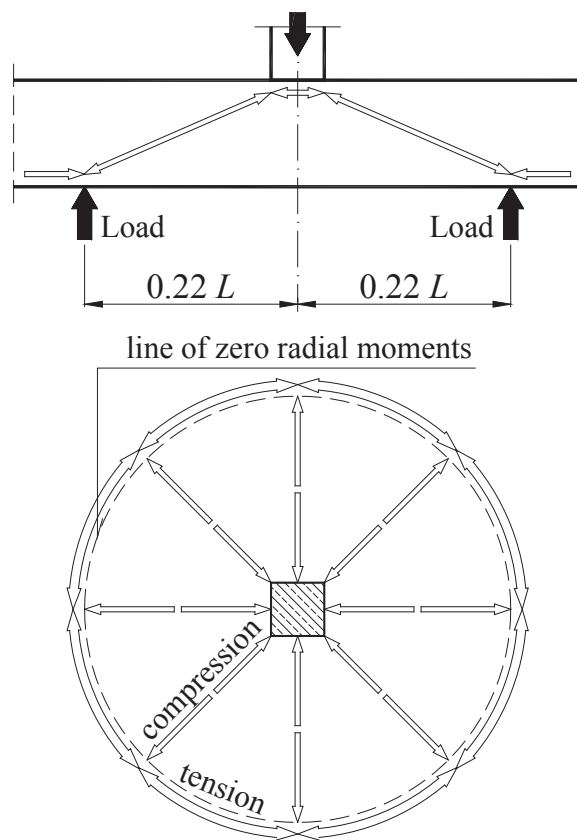


Fig. 16. Mechanism of tensile membrane action

Therefore, it should be noted that it is unlikely for membrane action to demonstrate the shield forces during the research [6] and [7]. Reach of the model outside the zone of zero radial moments was too small (Fig. 17), for the hindered punching zone to appear.

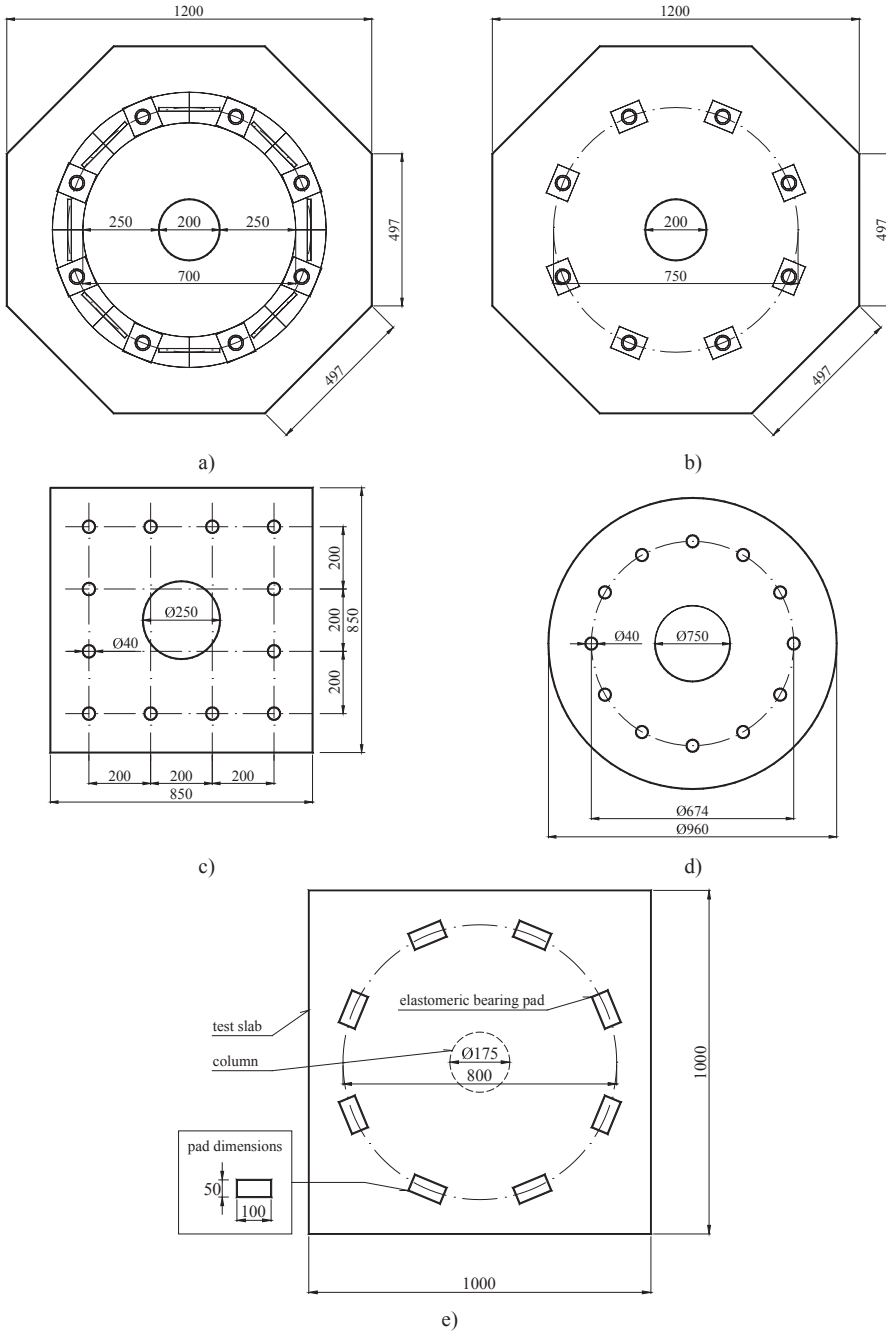


Fig. 17. Scheme of test stand: a) own research – the first series, b) own research – the second series, c) i d) Hallgren and other research [6], e) Timm research [7]

The appearance of the membrane action could be caused only by using longitudinal reinforcement. What is more, the effectiveness of this membrane action depends on the effectiveness of reinforcement anchorage at the edges of the models. The problem of different methods of anchorage of longitudinal reinforcement was investigated in the study [6], so some models with effective anchorage could be found above the theoretical curve of the ratio $v_{R,c}/v_{exp}$ shown in Fig. 15. According to the authors [6], the efficacy of longitudinal reinforcement in the thick elements is small. No space for anchoring the main reinforcement (such situation takes place in the pad footings) may result in failure due to the slide of the main reinforcement, which was already observed in Talbot research [3]. The important observation from the research is the mechanism of the destruction in punching of the thick reinforced concrete slabs, which in the ultimate limit state can demonstrate itself by radial cracks throughout the thickness of the concrete slab, as shown in Fig. 10 and 12. Breaking the model can be explained as the effect of transverse strain of the strut. Theoretical attempts to explain this phenomenon using the model S-T are shown in Rizk, Marzouk, Tiller study [11].

5. CONCLUSION

Results of the research and their preliminary analysis presented in the work allow to draw the following conclusions:

- shear slenderness is important for the punching capacity of reinforced concrete slabs,
- the restraint of column zone by the slab outside the zero line of the radial moments significantly increases the punching capacity – it is called ‘membrane action’,
- in the case of a membrane action, the curve in code according to the formula (2) is a safe approach
- using equation (2) in the case of the absence of membrane action, as it takes place in pad foundation, can be dangerous.

The research presented in this paper was funded by the Ministry of Science and Higher Education – a research project No. N N506 158440

REFERENCES

1. LAVROVICH J.S, McLEAN D.I: Punching Shear Behavior of Slabs with Varying Span-Depth Ratios. ACI Structural Journal, V.87, No 5, 507-512, September-October 1990.
2. EN 1992-1-1:2004 Design of concrete structures. General rules and rules for buildings.
3. TALBOT, A.: Reinforced Concrete Wall Footings and Column Footings. University Of Illinois Bulletin, Vol. X, N. 27, 1913.
4. RICHART, F.E.: Reinforced Concrete Wall and Column Footings, Journal of the American Concrete Institute, Vol. 20, 1948.

5. DIETERLE, H.: Zur Bemessung quadratischer Stützenfundamente aus Stahlbeton. DAFStb, Heft 387, Berlin, 1987.
6. HALLGREN, M., KINNUNEN, S., NYLANDER, B.: Punching shear tests on column footings. Nordic Concrete Research, Stockholm, 1998.
7. TIMM, M.: Durchstanzen von Bodenplatten unter rotationsymmetrischer Belastung, DAFStb, Heft 547, Berlin, 2004.
8. HEGGER, J., RICKER, M., SHERIF, A.G.: Experimental Investigations on Punching Behavior of Reinforced Concrete Footings, ACI Structural Journal, Vol. 103, No. 4, 604-613, July-August 2006.
9. HEGGER, J., HÄUSLER, F., RICKER, M.: Zur Durchstanzbemessung von ausmittig beanspruchten Stützenknoten und Einzelfundamenten nach Eurocode 2, Beton- und Stahlbetonbau, Vol. 103, No. 11, 727-734, November 2008.
10. RANKIN, G.I.B., LONG, A.E.: Predicting the enhanced punching strength of interior slab-column connections. Proc. of the Institution of Civil Eng., V. 82, Part 1, 1165-1186, December 1987.
11. RIZK E., MARZOUK H., TILLER R.: Design of Thick Concrete Plates Using Strut-and-Tie Model. ACI Structural Journal, Vol. 109, No. 5, 677-685, September-October 2012.

Received 11.02.2013

Revised 10.06.2013